This article has been accepted for publication in a future issue of this journal, but has not been fully edited. Content may change prior to final publication. Citation information: DOI 10.1109/JSEN.2018.2826547, IEEE Sensors Journal

Novel Ultrasound System with Intelligent Compensate Sensing for High Precision Measurement of Thin Wall Tube

Xiang Xiao[1], Bin Gao[1*], Gui Yun Tian[1, 2], Yi Cheng Zhang, Shu Chen

[1]School of Automation, University of Electronic Science and Technology of China, China

[2]School of Electrical and Electronic Engineering, Newcastle University, England, UK

*Corresponding author: bin_gao@uestc.edu.cn

***Abstract* —Ultrasound is widely used for measuring wall-thickness and diameter of tubes. All tubes are required to conduct the full profile of inspection to guarantee the quality by using an automatic Nondestructive testing system. However, most of the current ultrasonic testing works were done under the stationary condition for both specimen and probes with limited detection area. There exist challenges for providing a precisely measurement by approaching an automatic ultrasonic testing with high-speed inspection while it suffers the influence from temperature change of the water, mechanical vibration and tube deformation. In this paper, the spectral analysis of ultrasonic resonance was applied to measure the wall-thickness and diameter of the tubes. Besides, a novel intelligent compensation ultrasonic system with embedded strategy of self-organizing feature mapping (SOFM) artificial neural network is proposed to eliminate the interference under the condition of high-speed inspection. The experimental and comparison studies have been carried out. The corresponding results illustrate that the measurement precision of diameter and wall thickness can be effectively improved by using the proposed method.**

***Index Terms* — Thin wall-thickness, High precision, Nuclear tube, Artificial neural network, Ultrasound.**

NOMENCALATURE

Some notational symbols are listed below:

SOFM	Self-organizing feature mapping
NDT	Non-destructive testing
FFT	Fast Fourier Transform
EMAT	Electromagnetic acoustic transducer
URCAS	Ultrasonic reflection coefficient amplitude spectrum
SNR	Signal to noise ratio
IR	Infrared
EM	Expectation maximization
ANN	Artificial neural network
c_0	Ultrasonic wave velocity in water
c_1	Ultrasonic wave velocity in tube

I. INTRODUCTION

The zirconium alloy cladding tube is the first protection for the safety of the nuclear reactor. Nuclear fuel to the reactor is loaded into long tubes which are made from almost pure (98%) zirconium as it is practically transparent to various atomic particles. The zirconium alloy cladding tube not only acts as a containment and encapsulation to avoid the corrosion of the coolant and mechanical erosion but also seals the fission products and provides structural support for the fuel elements. Commonly, the diameter of zirconium alloy cladding tube is between 6~9mm, whereas the wall thickness is between 0.57~0.7mm. In the process of the tube production, the main types of defects are longitudinal cracks, transversal cracks, slag inclusion and unevenness of wall thickness or diameter. Once the transformation happened, it is a danger that they could become stuck in the graphite rings. On the other hand, the corrosion is activated in areas and it is mechanically damaged by the array supporting the fuel cassette in the flow of the hot water. As a result, the number of damaged and corroded zones has gradually increased [1].

Therefore, non-destructive testing (NDT) methods were developed to measure the wall thickness and diameter. These include visual examination, leak test, eddy current test and so on [3,6]. Kota Sasaki researched optimized microwave probes of excitation for measuring the wall-thickness of the metal pipes with an arbitrary diameter [11]. Marko Rakvin developed Computed Radiography to evaluate the pipe wall-thickness [2]. The IR thermography method was used to detect wall-thinning defects [5]. However, these methods can only detect wall thickness beyond 1mm. Compared with these methods, ultrasonic measurement of wall-thickness, distance and velocity attracts increasing attention in the areas of metals, composite materials and medical treatment of body structure. It has advantages of low cost, flexible operation, simple device and high safety. The ultrasonic wave propagation in the tube was studied by Mihai Valentin Predoi and M.S. Choi [7, 8]. Based on the time of flight principle of the ultrasonic wave, the thickness and diameter of zirconium alloy cladding tube can be measured [1]. However, the transducers should be placed inside the tube while it is hard to be operated and brought errors as well. When the thickness of specimen is less than 1mm, the time interval between pulse echoes is very short due to the fast acoustic velocity. In this case, precisely determining the time interval of pulse echoes requires a high time resolution of the transducer and the relevant device. This is because of the overlap of successive bottom echoes [14]. To overcome this challenge, in recent years, Dixon et al. [9] found that the thickness and the elastic modulus of an epoxy coating can be simultaneously obtained by means of ultrasonic bulk wave resonance technique based on the non-contact wide-band electromagnetic acoustic transducer (EMAT). It is able to detect the wall-thickness less than 1mm with the resonance technique. Y. Zhao developed an effective EMAT nondestructive method for simultaneous determination of coating thickness and ultrasonic longitudinal velocity via combining the URCAS with the inverse algorithm [10]. Jiao used time-frequency analysis to extract the film thickness from its reflection ultrasonic signals with wavelet transform method

This article has been accepted for publication in a future issue of this journal, but has not been fully edited. Content may change prior to final publication. Citation information: DOI 10.1109/JSEN.2018.2826547, IEEE Sensors Journal

[12]. Kai Zhang modeled the overlapped echoes and used EM algorithms to extract the interested echo to obtain the lubricant film thickness by using the ultrasonic spring model [13]. The ultrasonic resonance method based on spectral analysis was used for accurate thickness measurement of the irregular aluminum alloy sample [14].

However, there exist many impact factors would affect the measurement precision of the wall-thickness and diameter. Several methods have been reported for improving the precision of the measurement. The influence mechanism of the tube rotation method has been analyzed to improve transverse wall-thickness measurement [22]. The influence of lateral displacement of the transducer on the precision of thickness measurement has been analyzed by Sen CONG [14]. In order to enhance the SNR for the obtained ultrasonic signals, the signal processing using wavelet transform is developed [15]. However, the measurement precision is not only dependent on the elimination of the acquisition noise, but also depending on the variation of water temperature. Specifically, the acoustic velocity is the key parameter for measuring the diameter. Most of the previous works were done under the stationary condition for both specimen and the probes. It is not able to monitor the overall state of the tube. The detection area is limited. To measure the wall-thickness and diameter of the tubes precisely under the high-speed rotary automatic inspection is a challenge task. Since the vibration of the mechanical device could lead to the gradual temperature increment as the motor shaft is rotating at high-speed. In this work, the transducers are moving around the tube to cover 100% detection area at high-speed rotation and the novel intelligence compensation ultrasonic system with the embedded artificial neural network (ANN) is proposed. It enables us 1) to eliminate the influence of water temperature change on acoustic velocity; 2) to reduce the ultrasonic signal vibration under the high rotation speed; 3) to eliminate the influence from the tube deformation due to the gravity.

The rest of the paper is organized as follows: Section II discusses the principle of wall-thickness measurement by using resonance method. Specifically, the novel intelligence compensation ultrasonic system is proposed to reduce measuring errors. Section III describes the experimental setup and Section IV presents the experimental results and discussions. Finally, Section V concludes the works.

II. METHODOLOGY

A. Introduction of ultrasonic measurement of wall-thickness and diameter

In order to clearly interpret the ultrasonic testing of the water immersion, the schematic of the detection system is shown in Fig.1 (a). The controller drives the motor to make the tube move forward and the transducer is driven to rotate at the same time to make a spiral relative motion between the tube and the transducer. The ultrasonic instrument transmits square waves to excite the transducer and receive echo signals. The so-called square wave is not a signal with duty cycle 1:1. Actually, it is a pulse signal. The pulse signal is used to excite the ultrasonic transducer with a voltage or current that has an abrupt change for a certain period of time. Fig.1 (b) presents the side view of the inspection system when the ultrasonic wave is incident perpendicularly to the surface of the specimen, the reflection and transmission will occur in the inhomogeneous interface. In comparison, the traditional wall thickness measurement method is based on the calculation of time of flight between the top and bottom echoes. Assuming that the ultrasonic pulse duration is Δt, the round-trip time of the medium that passes through the tube is $\Delta\tau$, when the wall thickness of the tube is large as $\Delta\tau>\Delta t$, the echoes between top and bottom interface can be distinguished easily as shown in Fig.1 (c). When the wall-thickness of the tube is reduced to $\Delta\tau<\Delta t$, the echoes between top and bottom interface is too close that the echoes signal is overlapped as shown in Fig.1 (d). In this situation, it is difficult to find the characteristics of the two echoes' signals through time domain analysis. In addition, when one part of the waves passes through the top interface and interferes with those reflected at the bottom, the stationary waves are produced because of the same frequency, amplitude and opposite propagation directions. Therefore, in this work, the resonance method based on FFT spectral analysis was used to measure the wall-thickness of the tube.

The corresponding resonance information which hides in the A-scan signal is extracted by the digitization ultrasonic detection system. Thus, we can obtain a series of equations by different resonance frequencies from f_m, $\cdots$,f_{n-1},f_n as shown in Fig.1 (e). It is the result of the spectrum analysis of the original signal. When the wall-thickness d is equal to integer times of half-wavelength of the ultrasonic wave ($d=n\lambda/2$, n is an integer, λ is the wavelength of the ultrasonic wave in the specimen), stationary wave and resonance will occur in the direction of thickness in the tube. The measurement of wall thickness d can be obtained [14] as

$$d = \frac{c_1}{2(f_n - f_{n-1})} \tag{1}$$

where f_{n-1} and f_n are the two resonance frequencies. According to the wave theory, the relationship between the wavelength λ, frequency f, and ultrasonic velocity c is $f = c/\lambda$. Taking ultrasonic velocity c_1, the n-th and m-th resonance frequencies into wave equation, the n-th and m-th wave equations are obtained as $f_n = c_1/\lambda_n$ and $f_m = c_1/\lambda_m$. Taking them into Eqns.(1), the Eqns.(2) can be obtained:

$$d = \frac{(m-n)c_1}{2(f_m - f_n)} \tag{2}$$

where f_n and f_m are the n-th and m-th resonance frequency respectively. c_1 is ultrasonic wave velocity in the tube.

Then Eqns.(2) can be rewritten as, namely:

$$d = \frac{c_1}{2\Delta f} \tag{3}$$

where the $\Delta f = \frac{(f_m - f_n)}{(m-n)}$ is the mean difference of frequency.

Thus, according to Eqns. (3), the wall-thickness can be acquired by measuring the harmonic frequency by analyzing the spectrum with prior knowledge of the propagation wave velocity c_1 in the specimen.

Since the ultrasonic wave is perpendicular to the surface of the top interface as shown in Fig.1 (b), the ultrasonic wave propagates in water firstly and then penetrates the tube. Therefore, the water column d_1 from the transducer to the surface of the top interface of the tube can be calculated as

$$d_1 = \frac{1}{2} c_0 t \tag{4}$$

where t is the time of interfacial wave acquired by A-scan signal. It is total time for transmitting wave from the

This article has been accepted for publication in a future issue of this journal, but has not been fully edited. Content may change prior to final publication. Citation information: DOI 10.1109/JSEN.2018.2826547, IEEE Sensors Journal

transducer and reflecting back from surface of the tube to instrument. Therefore, d_1 is the distance from the transducer to the surface of the tube. The variable d_1 is also called water column.

According to the geometric relationship as shown in Fig.1 (b), the diameter of the tube can be calculated by using the following expression.

$$r = 2 \times (d_t - d_1 - d) \quad (5)$$

where r is the diameter of the tube, d_t is the distance from the transducer to the center of the tube, it can be easily measured by applying the mechanical measurement.

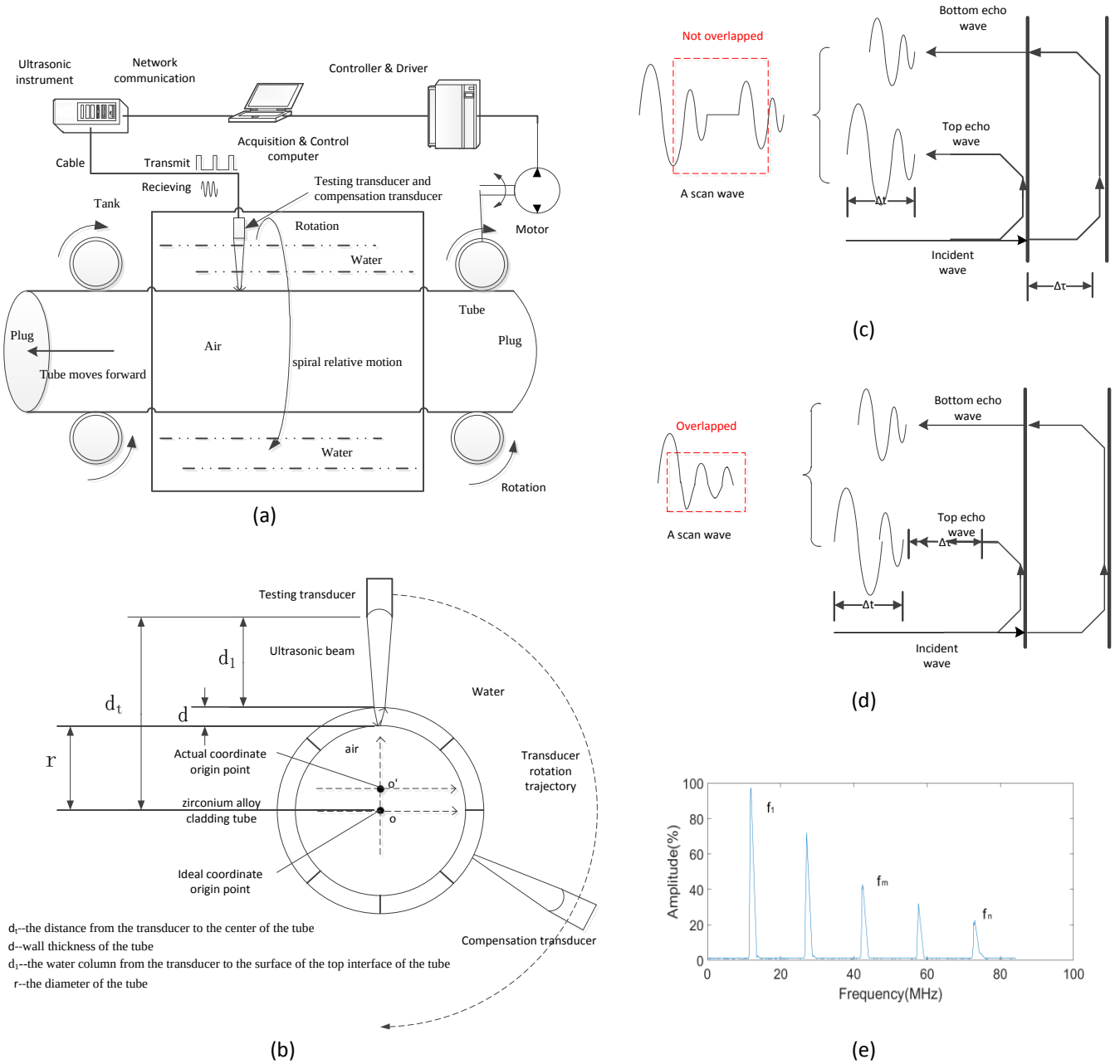

Fig.1: (a) The detection system schematic; (b) the side view of inspection system; (c) the echoes can be distinguished; (d) the echoes overlapped; (e) the schematic of resonance frequencies

If the measured t with water velocity c_0 is under the known water temperature, mechanical distance d_t and measured wall-thickness d, then the diameter of the tube will be obtained according to Eqns. (4)~(5). However, the ultrasonic velocity is not a constant value due to the temperature change. Besides, the t in Eqn. (5) measured by processing ultrasonic signal is affected by tube deformation and mechanical vibration.

B. Improvement of precision methodology

It is necessary to find a feasible method to solve these problems as mentioned in Session A. In this work, the measuring structure of the intelligence compensation ultrasonic system with embedded ANN has been proposed to improve the measurement precision. The working procedure can be divided into two steps as shown in Fig.2. The first step is building the compensation transducer structure which has a prior experience of the surface time of the testing transducer

This article has been accepted for publication in a future issue of this journal, but has not been fully edited. Content may change prior to final publication. Citation information: DOI 10.1109/JSEN.2018.2826547, IEEE Sensors Journal

with circumferential location. The second step is a testing process which uses compensation transducer structure with embedded ANN to eliminate the interference from water temperature, signal vibration and correct effects of tube deformation. During the testing process, the ultrasonic signal of the testing transducer and intelligence compensation transducer are hybridizing together to obtain the measurement of wall-thickness as well as refining the water column of the testing transducer. Finally, the thickness and diameter are determined according to Eqns. (3), (5) and (7).

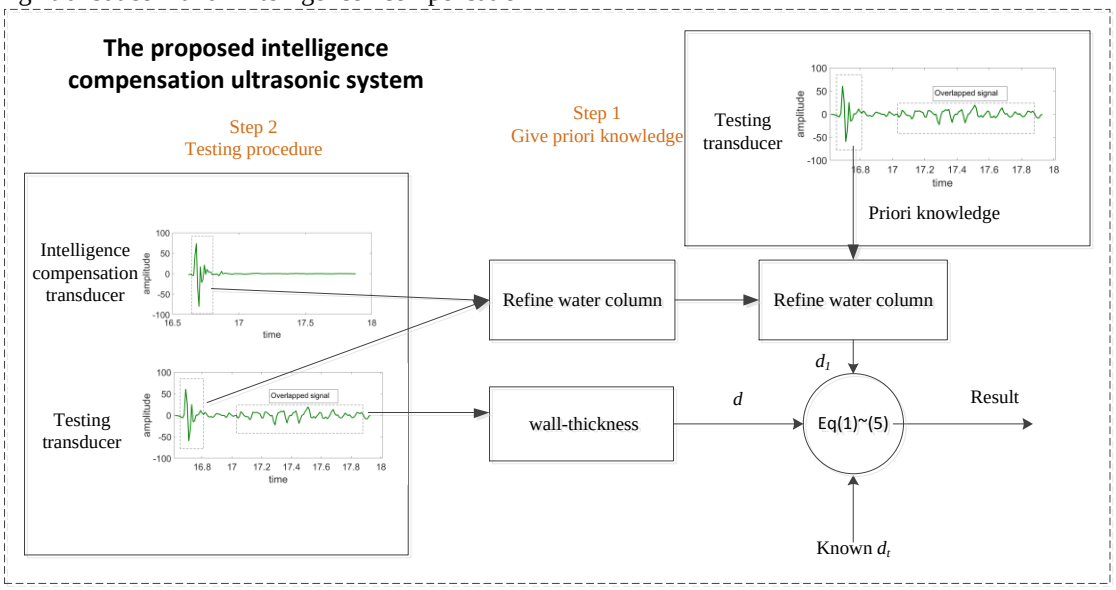

Fig.2 the proposed intelligence compensation ultrasonic system

1) Eliminate the interference from water temperature change

In the process of measurement, the transducer rotates around the center of the tube as shown in Fig.1, respectively. During the propagation of ultrasonic waves, the waves pass through a medium of water and then incident into the tube vertically. However, the change of the water temperature and tube material leads to the variation of time of flight. The Eqns. (1) ~ (5) indicate that ultrasonic velocity is one of the key factors affecting the precision of measurement. In the continuous rotation of the transducer, the water and tube temperature will gradually rise due to the friction between the transducer and water, the friction of the transmission mechanism and the heat conduction of the mechanical system heat dissipation. The relationship between ultrasonic velocity and temperature variations can be obtained by thermocouple [17]. In the traditional method, the correction of ultrasonic velocity depends on this relationship table by assembling temperature sensor.

However, it still exists errors as the transducer is rotating in the tank filled with water. The temperature is not always the same since the mixing of the water current is not complete. In addition, the closer to the motor driving shaft, the higher temperature the water has. The gradient difference in temperature exists in the water tank. Therefore, the temperature acquired by the thermocouple sensor does not represent the actual temperature where the transducer located. In different media, the effect of temperature change on ultrasonic wave velocity is different. The ultrasonic wave propagates in water is more sensitive to temperature than in the steel. When the water temperature rises from 0℃ degrees to 45℃ degrees, the change of wave velocity is large (up to 89m/s). As the water temperature rises, the ultrasonic velocity increases logarithmically. On the contrast, as the steel temperature rises, the ultrasonic velocity decreases linearly. When the steel temperature rises from 0℃ degrees to 45℃, the change of wave velocity is small, only 23m/s. In this situation, the error of the ultrasonic velocity in steel can be ignored because of the small variety range. Since the wall-thickness is very thin (less than 1mm), the propagation time in the tube will be very short.

In the proposed work, the novel intelligence compensation ultrasonic system was developed to eliminate the variation of ultrasonic velocity in water c_1 as shown in Fig.3. It is made of a moving target, a fixing target and a transducer named compensation transducer that is rotating around the target. The intelligence compensation transducer is aiming at a mechanical structure that is composed of a circular reflector and a curved reflector while it is rotating around the mechanical structure. In the mechanical structure, the curved reflector keeps a distance from the circular reflector. However, the center of the curved and circular reflector is in the center of the transducer rotation. In other words, with respect to the transducer, the circular reflector is a fixed target and the curved reflector is a moving target. The time of flight from the transducer to the fixed target T_f and to the moving target T_m can be measured by using A-scan signals. In order to reduce the interference from temperature on the ultrasonic velocity at different positions of the transducer, all the time of flight will be recorded per rotation. During each rotation, there exist two statuses. When the ultrasonic beam is close to the left edge of the moving target, it begins to enter the first status as shown in Fig.3 (a). At this moment, ultrasonic waves will be fully reflected from the moving target. The time of flight T can be measured by interfacial echo of the A-scan signals as shown in Fig.3 (b) with red color line. In this situation, T is equals T_m ($T = T_m$) where T_m is the time of flight from transducer to the moving target. With the rotation of the transducer, the signal

This article has been accepted for publication in a future issue of this journal, but has not been fully edited. Content may change prior to final publication. Citation information: DOI 10.1109/JSEN.2018.2826547, IEEE Sensors Journal

will be remained for a period of time due to the width of the moving target. When the ultrasonic beam is moving out of the right edge of the moving target, it begins to enter the second status as shown in Fig.3 (a). The ultrasonic waves will be fully reflected back from the fixed target. The time of flight T can be measured by the interfacial wave of A-scan as shown in Fig.3 (b). In this situation, T equals T_f whereas it is larger than T_m ($T_m < T_f$), where T_f is the time of flight from the transducer to the fixed target. In the same way, the signal is retained for a period of time until it enters the first status in the next cycle. If the time of flight T is taken as a y-axis and the sampling sequence is used as an x-axis, then as the transducer rotates, T will turn the status between the first status and the second status periodically and alternatively as shown in Fig.3 (c). One of the statuses could be the trigger signal as the start and end position per rotation. Therefore during one rotation, the average time of flight T can be calculated as

$$T_{ref}^{n} = \frac{\sum_{i=N\times n}^{N\times n+N-1} T_{ref}^{i}}{N}, \quad T_{ref}^{i} > T_m \tag{6}$$

where T_{ref}^{n} is the compensation time of flight for rotation n, T_{ref}^{i} is the time of flight determined in the previous section, n is the index of the rotation number, N is the number of firings per rotation, i is the index of A-scans. The variation of temperature has same impact on compensation transducer and testing transducer since both of them have the same axial position and moving at the same time. Then the water column can be obtained as

$$d_1 = \frac{T_i}{T_{ref}^{n}} \times D_{ref} \tag{7}$$

where D_{ref} is the distance of compensation transducer to the fixed target, T_i is the index of the measured time of flight. According to Eqn. (7), the water temperature change will be eliminated and no more temperature sensors will be required.

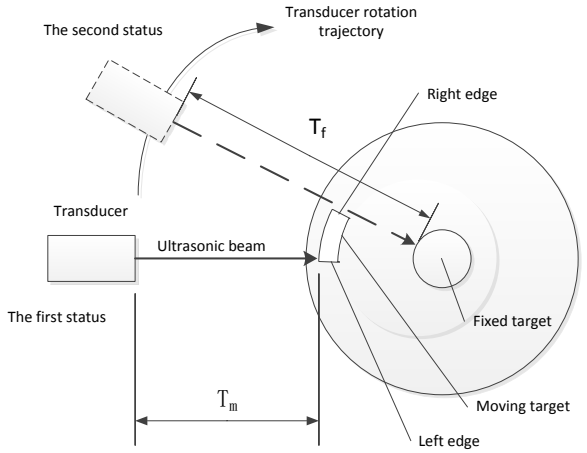

(a)

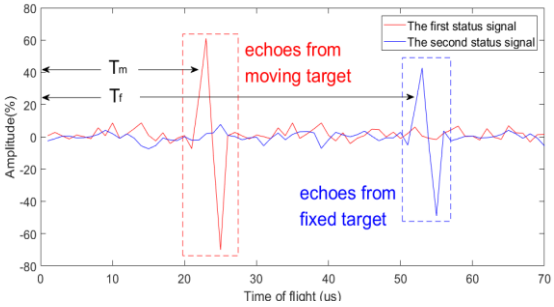

(b)

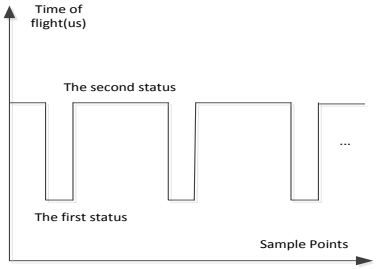

(c)

Fig.3: (a) The compensation transducer is introduced to eliminate the variation of ultrasonic velocity in water; (b) The original echoes of the first and second status; (c) The periodical and alternative status.

2) Eliminate the influence of deformation and mechanical vibration

The tube will be deformed under the action of gravity due to its thin wall-thickness. In this case, the center of rotation will rise as shown in Fig.1 (b) and the actual center arises from the ideal point *o* to the actual point *o'*. The transducer around the tube rotation trajectory is not a circle, but an ellipse. Thus, it is difficult to measure the degree of the deformation. If we carried out the water column at the rotation sequence axis, the signal will look like a sinusoidal signal as shown in Fig.4. The vertical ordinate represents the measured distance from the transducer to the top interface of the tube by using Eqn. (7). Unfortunately, what makes the worse is the mechanical vibration that will result in the shaking of the transducer during the high-speed rotation measurement. The ultrasonic signal will be affected by the vibration. The interference signal will be superimposed on the sinusoidal signal. In order to reduce the influence of deformation due to the gravity and mechanical vibration, the model between the water column and circumferential position of the transducer was established. According to this, the SOFM neural network is embedded to estimate the true value d_1 in every acquisition point per rotation rather than the measured value d_1, where d_1 is the water column.

This article has been accepted for publication in a future issue of this journal, but has not been fully edited. Content may change prior to final publication. Citation information: DOI 10.1109/JSEN.2018.2826547, IEEE Sensors Journal

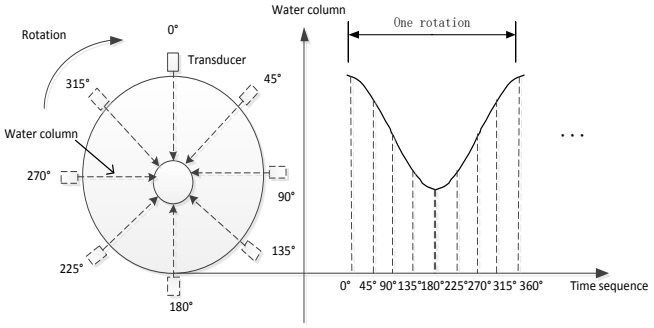

Fig.4 the water column carried out at time sequence

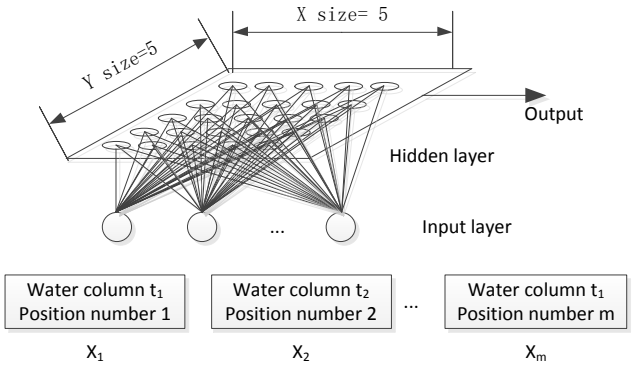

Fig.5 the structure of SOFM Neural Network

SOFM ANN is a self-learning and self-organizing network without supervising composed by connecting the whole neurons array. The SOFM network can map any dimension input model into an output layer as a one-dimensional or two-dimensional graph, and maintain its topological structure. The network can make the weight vector space converge to the probability distribution of the input pattern by repeated learning of input patterns, probability preserving. The Fig.5 shows the structure of the SOFM network. The algorithm is described as follows [21, 23, 24]:

The learning rate is initialized as $\eta(0)=\{0\leq\eta\leq1\}$, the weight w_{ij} is initialized randomly within the range [0,1], and the neighborhood initial value $N_g(0)$. Thus, the learning model and normalize the input vector p_k to p_n^k are selected as

$$p_k^* = \frac{(p_1^k, p_2^k, \ldots p_n^k)}{\sqrt{(p_1^k)^2+(p_2^k)^2+\cdots+(p_n^k)^2}} \tag{8}$$

The Euclidean distance is calculated between W_j^* and p^*:

$$W_j^* = \frac{(w_{j1}, w_{j2}, \ldots w_{jn})}{\sqrt{(w_{j1})^2+(w_{j2})^2+\cdots+(w_{jn})^2}} \tag{9}$$

$$d_j = \sqrt{\sum(p_i^* - W_{ji}^*)^2} \qquad j = 1,2,\ldots,m \tag{10}$$

The winning neuron is found according to minimum dg:

$$d_g = \min\left[d_j\right] \quad j = 1,2,\ldots,m \tag{11}$$

The connection weights between the selected neurons and neighboring neurons are adjusted:

$$W_{ji}^*(\mathrm{t}+1) = W_{ji}^*(\mathrm{t}) + \eta(t)^*\left[p_i^* - \mathrm{W}_{\mathrm{ji}}^*\right] \quad j \in N_g(t) \tag{12}$$

Once a new sample enters, the progress starts repeating until the learning model is all available to the network. Thus, the specific procedure of the proposed method can be summarized as follows:

a) Prior to the starting test, the water column at each position of the standard tube is collected per rotation. The inputs of the neural network are rotary position and the corresponding water column. The SOFM neural network is trained. Thus, the average water column data at every position in numbers of rotation can be obtained as.

$$T_{est}^i = \frac{\sum_{j=1}^k t^i}{k} \qquad i = 1,2,\ldots m \tag{13}$$

where i is the index of position per rotation, j is the index of rotation, k is the number of total rotation. Then the average of water column $T_{\mathrm{est}}^{\mathrm{i}}$ can be written as a vector, this vector is estimated data to replace the measured data.

$$T_{est}^i = (t_{est}^1, t_{est}^2, \ldots, t_{est}^i) \tag{14}$$

b) The SOFM neural network is embedded to determine the measured water column within the system error under a certain rotational speed condition.

c) When the test started, the water column of the measuring tube at each position can be acquired per rotation. These data are fed to the trained SOFM neural network to automatically classify the result.

d) According to the result of classification, the measured water column which belongs to the system error is determined. If it belongs to a system error, then the water column data will be replaced by known T_{est}^i, if not, that means the data are reserved for calculating $T_{\mathrm{kpt}}^{\mathrm{i}}$.

e) Finally, the T_{est}^i or T_{kpt}^i will be used to calculate the tube diameter according to Eqns. (3) and (5).

III. EXPERIMENTS SETUP

The specimens are made by the manufacturers of zirconium alloy cladding tubes which are used for the nuclear power plant. The material of the tube is 316Ti alloy with Φ9.677 diameter and 0.677mm wall-thickness. The specimens are divided into three parts. One is standard tube used for calibration and this kind of specimen is calibrated by the National Measurement Institute. The other two with a section of worn zone separately are used for testing. The wall-thickness of the testing sample one has thinned 0.02mm during worn zone. The diameter is 9.657mm and the wall-thickness is 0.657mm as shown in Fig.6 (a). The wall-thickness of testing sample two has thinned 0.05mm during worn zone. The diameter is 9.627mm and the wall-thickness is 0.627mm as shown in Fig.6 (b).

In the experiment, the testing tube was submerged in water and moving from right to left through the detecting device while the transducers are rotating at the same time. In order to prevent water from flowing into the tube, both ends of the tube are sealed with plugs as shown in Fig.1. Though the seal is turning the tube into an echo chamber, the ultrasonic wave cannot propagate into the air due to the extremely high frequency (15MHz). The reason can be drawn as the steel acoustic impedance is significantly different from the air acoustic impedance. Therefore, when the ultrasonic wave propagates from steel to the air, the wave will be fully reflected by the interface between the steel and air. The Fig.6 (c) (d) shows the testing system device which consists of the transducer assembly, motors, retarder, rotor, and so on. Fig.6 (c) shows the overview of the proposed ultrasonic system. The transducer assemblies are covered for the protection because of high-speed rotation. Fig.6 (d) shows the details after the protective cover is removed. In the process of measurement,

This article has been accepted for publication in a future issue of this journal, but has not been fully edited. Content may change prior to final publication. Citation information: DOI 10.1109/JSEN.2018.2826547, IEEE Sensors Journal

the rotor drives the probe assembly to rotate, and the tube passes through the detecting device from right to left to complete the full volume inspection. The inner part of the rotating device is a hollow, and it is full of water while detecting. The transducer is a kind of immersion focusing probe with high working frequency up to 15MHz. The focal distance and focal point diameter of the transducer are 18mm and 0.5mm respectively. The ultrasound data is acquired by multi-channel automatic equipment with 100MHz acquisition rate and 5KHz pulse-repetition frequency under the 6000RPM rotation speed.

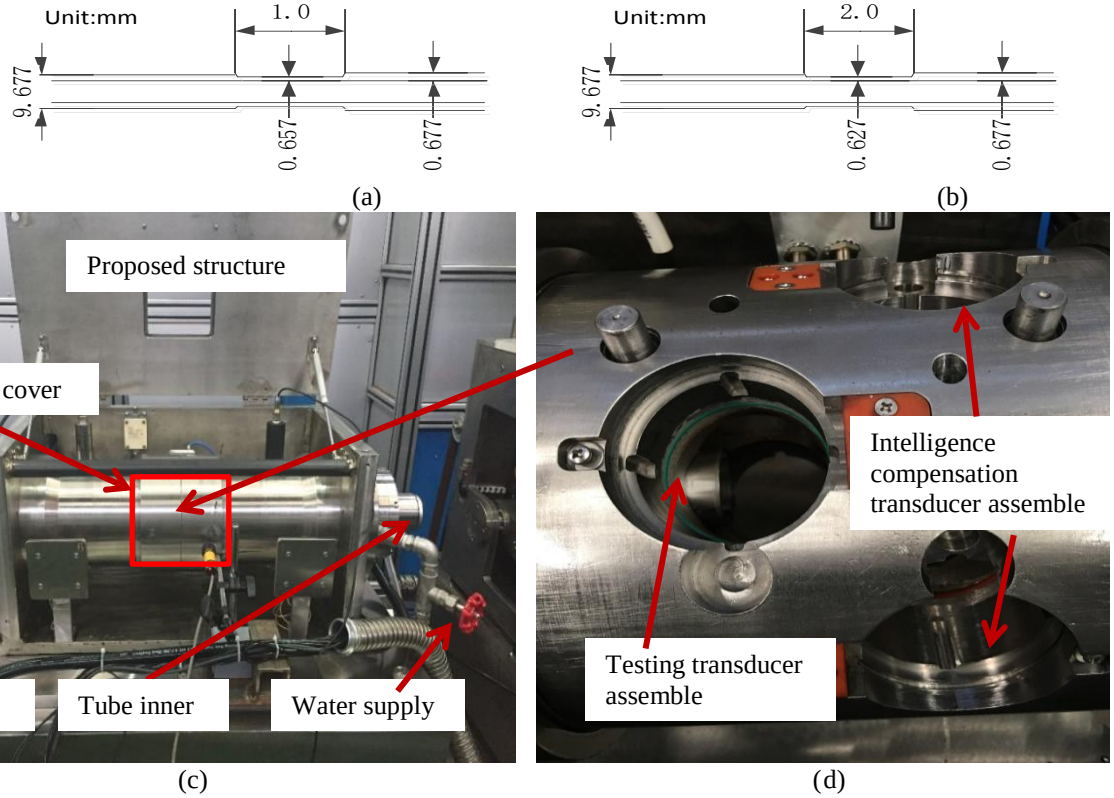

Fig.6: (a) the testing sample of number one; (b) the testing sample of number two; (c) the overview of proposed detecting device; (d) the detail of proposed detecting device.

IV. RESULTS AND DISCUSSION

In order to clearly explain the proposed method, the steps of the data processing are listed as follows:

1) The original A-scan signal is acquired from the instrument as shown in Fig.7 (a).

2) The overlapped echoes of A-scan signal are transformed into resonance frequency signal as shown in Fig.7 (b).

3) According to Eqns. (1) ~ (3), the wall-thickness *d* can be obtained.

4) The water column of the reference transducer and the testing transducer are obtained respectively from the interfacial wave of the original A-scan signal.

5) According to Eqns. (6) ~ (7), the water column of the testing transducer is refined. The Fig.7 (f) shows the result without elimination of the variation influence from the ultrasonic velocity in water.

6) The results of the step 5th are the inputs for ANN learning and testing to eliminate the influence of deformation and mechanical vibration according to Eqns. (8) ~ (14). The result of the comparison of the data collected in the normal zone before and after the classification is shown in Fig.7 (c) and (d). The classification results of the wear zone and the normal zone are shown in Fig.7 (e).

7) Finally, the diameter can be calculated by the results of step 5th and 6th according to Eqns. (4) ~ (5). These results and discussion are shown in Fig.7 (f) ~ (j).

The specimen with the known worn zone is tested. Fig.7 (a) shows the measured A-scan wave in the time domain. It can be shown that the signal with high amplitude at the beginning is the ultrasonic wave interacting with the top interface of the tube. Besides, the oscillatory wave is the multiple back wall echoes which are the results from the multiple wave reflections between the top and the bottom interfaces. Thus, the oscillatory wave is the resonance wave. It can be clearly seen that the amplitude of the surface is much higher than the resonance wave. It is owing to the energy attenuation of the ultrasonic wave propagation in the material. In addition, the reflected echo and the forward propagating wave will interfere with each other which will lead to the amplitude decrease.

In this work, after the time of flight at 50us, the gain is improved 0.1dB in order to prevent the attenuation of the signal so that the frequency information is lost. Therefore, it can be found that the amplitude is bigger after the time of flight at 50us from Fig.7 (a). The interface wave is used for calculating diameter and the resonance wave is used for

This article has been accepted for publication in a future issue of this journal, but has not been fully edited. Content may change prior to final publication. Citation information: DOI 10.1109/JSEN.2018.2826547, IEEE Sensors Journal

calculating wall-thickness. Fig.7 (b) shows the FFT wave transformed from the resonance wave whose surface wave was cut off. Three resonance frequencies (f_1, f_2, f_3) can be clearly read from the amplitude spectrum. According to Eqn. (3), the wall-thickness can be calculated.

The time of flight of the surface wave is used for measuring water column. The data are recorded under the condition of the transducer at 6000 rotation per minute. The Fig.7(c) (d) is the result of the comparison of the data collected in the normal zone before and after the classification. In the Fig.7 (c), there is blurred signal mixed in the water column signal of six rotations. The blurred signal of the curve is caused by mechanical vibration due to shaking of the transducers. It shows the water column trajectory without SOFM neural network classification. The six peaks represents six rotations data. The time of flight of the interface wave ranges from 25.62us to 26.19us according to the curve. The Fig.7 (d) shows the result of SOFM neural network classification. It can be clearly seen that the blurred signal caused by mechanical vibration is reduced. The water column data have been replaced by known T_{est}^{i} . The precision is better than the water column without classification. The Fig.7 (e) shows the classification results of the wear zone and the normal zone. According to the results, the data with black color is similar to the data acquired by standard tube (known T_{est}^{i}). On the other hand, the data marked with red color shows significant differences from the data acquired by standard tube. Therefore, the data in this rotation are reserved for calculating $T_{\mathrm{kpt}}^{\mathrm{i}}$. This indicates that the worn zone exists.

Fig.7 (f) ~ (h) shows the comparison of the measurements taken with traditional method and the proposed method for the tested sample number one. Fig.7 (f) shows the diameter result of the whole tube before using the proposed method. The result is getting down gradually due to the rise of the temperature from 25℃ to 45℃ and the vibration influence exists at the same time. Fig.7 (g) and (h) shows the measurement of wall-thickness and diameter result of the whole tube, respectively by using the proposed method. When the ultrasonic wave is scanning at the worn zone, both wall-thickness and diameter curves are indicated. The oscillatory curve indicated that the vibration cannot be eliminated and the precision is improved up to 0.09%. Table I shows the measurement result of wall-thickness and diameter of the whole testing tube. Compared with the traditional method, the result is improved 334.9um. It indicates that without proper calibration, the minimum result will lose precision with an increased temperature. The result indicates that the maximum wall-thickness deviation between the measured value and the real value is 9um and the maximum diameter deviation between the measured value and the real value is 3.7um.

Fig.7 (i) (j) shows the measurement of the test sample two by using the proposed method. Fig.7 (i) shows the measurement of wall-thickness of the whole tube and Fig.7 (j) shows the diameter measurement result of the whole tube. Table II shows the measurement results. Compared with the traditional method, the result is improved 0.9um. The maximum wall-thickness deviation between the measured value and the real value is 4um and the maximum diameter deviation between the measured value and the real value is 9um.

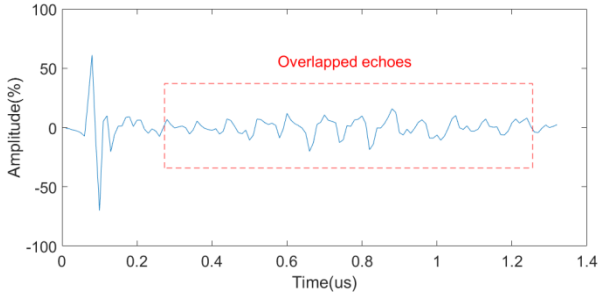

(a)

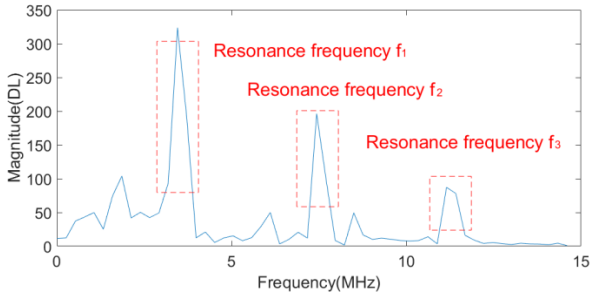

(b)

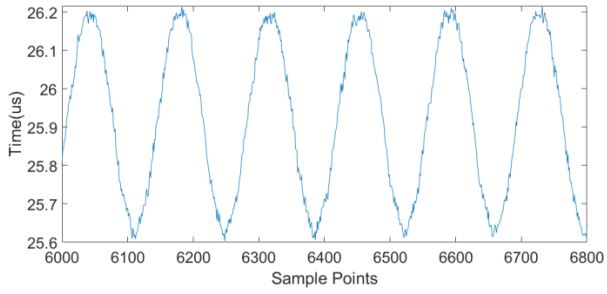

(c)

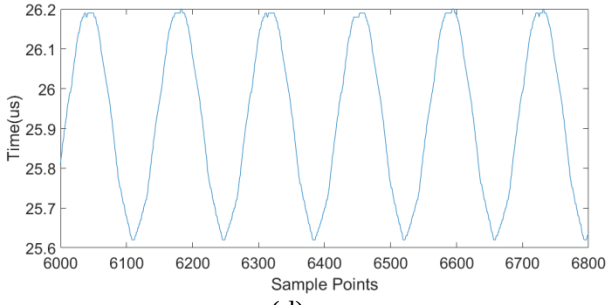

(d)

This article has been accepted for publication in a future issue of this journal, but has not been fully edited. Content may change prior to final publication. Citation information: DOI 10.1109/JSEN.2018.2826547, IEEE Sensors Journal

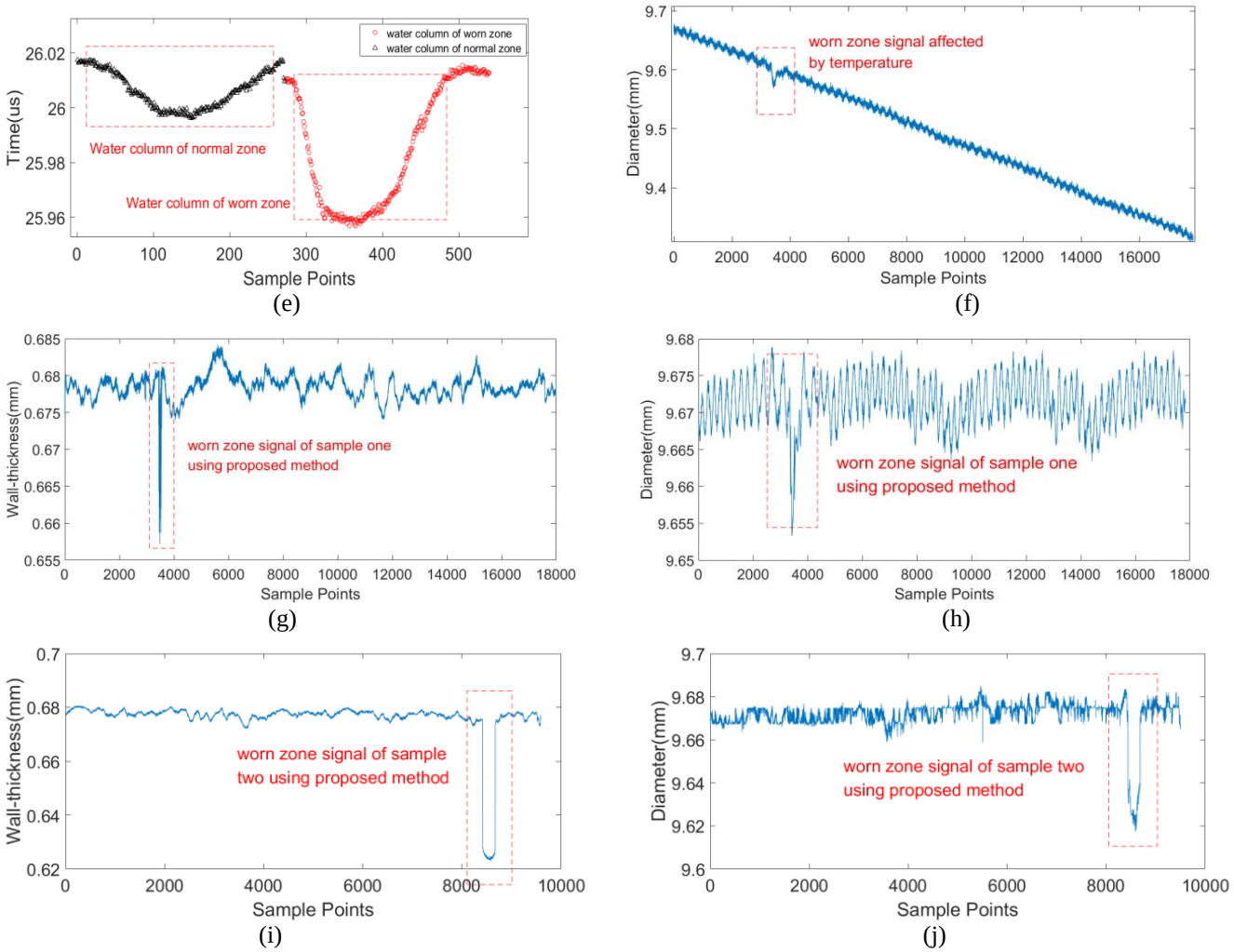

Fig.7: (a) Measured A-scan signal; (b) Resonance frequencies signal; (c) the data of six rotations before classification; (d) the data of six rotations after classification ;(e) The classification results of the wear zone and the normal zone; (f) the diameter result of the whole tube about sample one before using the proposed method; (g) the wall-thickness result of the whole tube of the sample one; (h) the diameter result of the whole tube after using the proposed method of the sample one; (i) the wall-thickness result of the whole tube about sample two;(j) the diameter result of the whole tube about sample two

Table I: The result of testing sample one

	Ground truth	Measured value (traditional method)	Measured value (proposed method)	Compare with traditional method	Compare with ground truth (relative error)
Whole tube wall-thickness	0.677mm	× × ×	Max:0.684mm Mean：0.6782mm Min：0.6567mm	× × ×	0.7%
Worn zone wall-thickness	0.657mm	×	0.6567mm	×	0.04%
Whole tube diameter	9.677	Max: 9.6780mm Mean: 9.4940mm Min: 9.3085mm	Max: 9.6789mm Mean: 9.6716mm Min: 9.6533mm	1.7um 177.5um 334.9um	0.05%
Worn zone diameter	9.657	9.6333mm	9. 6533mm	-70um	0.04%

Table II: The result of testing sample two

	Ground truth	Measured value (traditional method)	Measured value (proposed method)	Compare with traditional method	Compare with ground truth (relative error)

This article has been accepted for publication in a future issue of this journal, but has not been fully edited. Content may change prior to final publication. Citation information: DOI 10.1109/JSEN.2018.2826547, IEEE Sensors Journal

Whole tube wall-thickness	0.677mm	× × ×	Max: 0.6806mm Mean：0.6760mm Min：0.6230mm	× × ×	0.1%
Worn zone wall-thickness	0.627mm	×	0.6235mm	×	0.5%
Whole tube diameter	9.677	Max: 9.6722mm Mean: 9.4940mm Min: 9.2963mm	Max: 9.6850mm Mean: 9.6715mm Min: 9.6174mm	12.8um 177.5um 321.1um	0.05%
Worn zone diameter	9.627	9.2963mm	9.6174mm	321.1um	0.09%

Note '×' denotes the thickness cannot be measured by traditional method.

V. CONCLUSION AND FUTURE WORK

In this paper, a novel intelligence compensation ultrasonic system for wall-thickness and diameter measurement of the zirconium alloy cladding tube has been proposed. A deep analysis regards to the genesis of system error has been presented. The verification experiments have been conducted to validate its detection precision. Several conclusions can be drawn: i). the proposed system enables us to eliminate the change of ultrasonic velocity caused by water temperature variation which improves the detection precision. ii). the proposed system reduces the influence of tube deformation due to gravity so that the detection precision is improved. iii). the proposed system is able to reduce the effect from the signal vibration caused by the mechanical vibration so that the detection precision is improved. The wall-thickness measurement precision can be raised up to 0.5% and the diameter measurement precision can be raised up to 0.09%.The measuring diameter precision of the proposed method is 2.5% higher than that of the traditional method. Future work will carry out the detection with higher rotation speed that is faster than 8500RPM.

VI. ACKNOWLEDGEMENT

The work was supported by National Natural Science Foundation of China (No. 61401071, No. 61527803), Supported by NSAF (Grant No. U1430115) and EPSRC IAA Phase 2 funded project: "3D super-fast and portable eddy current pulsed thermography for railway inspection" (EP/K503885/1)

REFERENCES

[1] R. Kažys, L. Mažeika, R. Šliteris, A. Vladišauskas, K. Kundrotas. "Ultrasonic measurement of zirconium tubes used in channel-type nuclear reactors." NDT & E International, Volume 29, Issue 1, February 1996, Pages 37-49.

[2] Marko Rakvin, Damir Markučič, Boris Hižman. "Evaluation of Pipe Wall Thickness based on Contrast Measurement Using Computed Radiography (CR)." Applied Optics 55.34 (2016): D46-D53. Procedia Engineering, Volume 69, 2014, Pages 1216-1224

[3] D.S. Setty, K. Kapoor, N. Saibaba. "Nuclear fuel cycle - developments and challenges in fuel fabrication technology in India." Progress in Nuclear Energy, In press, corrected proof, Available online 18 March 2017.

[4] WANG Fu-xi, ZHOU Xiao-feng, E Nan, LI Bin. "Application of phased array ultrasonic testing technology on inspection of titanium thick welds ". The Chinese Journal of Nonferrous Metals, 2010,20(s1): s964−s966.

[5] Jin Weon Kim,Kyung Won Yun,Hyun Chul Jung. "Investigation of optimal thermal injection conditions and the capability of IRthermography for detecting wall-thinning defects in small-diameter piping components". Nuclear Engineering and Design, Volume 262, September 2013, Pages 39-51

[6] P. Barat, B. Raj, D.K. Bhatracharya. "A standardized procedure for eddy-current testing of stainless steel, thin-walled nuclear fuel element cladding tubes.". NDT International, Volume 15, Issue 5, October 1982, Pages 251-255

[7] Mihai Valentin Predoi, Cristian Cătălin Petre. "Multimode wave propagation in immersed pipes." Materials Today: Proceedings, Volume 3, Issue 4, 2016, Pages 1135-1138.

[8] M.S. Choi, H.C. Kim, M.S. Yang. "Propagation characteristics of elastic circumferential waves in nuclear fuel cladding tubes." Ultrasonics, Volume 30, Issue 4, 1992, Pages 213-219.

[9] Dixon S, Lanyon B, Rowlands G. Coating thickness and elastic modulus measurement using ultrasonic bulk wave resonance. Appl. Phys. Lett. 2006; 88:1–3.

[10] Y. Zhao, L. Lin, X.M. Li, M.K. Lei. "Simultaneous determination of the coating thickness and its longitudinal velocity by ultrasonic nondestructive method." NDT & E International, Volume 43, Issue 7, October 2010, Pages 579-585.

[11] Kota Sasaki, Linsheng Liu, Noritaka Yusa, Hidetoshi Hashizume. "Optimized microwave excitation probe for general application in NDT of wall thinning in metal pipes of arbitrary diameter." NDT & E International, Volume 70, March 2015, Pages 53-59.

[12] Jingpin Jiao, Wenhua Liu, Jie Zhang, Qiang Zhang, Bin Wu. "Time–frequency analysis for ultrasonic measurement of liquid-layer thickness." Mechanical Systems and Signal Processing, Volume 35, Issues 1–2, February 2013, Pages 69-83.

[13] Kai Zhang, Qingfeng Meng, Tao Geng, Nan Wang. "Ultrasonic measurement of lubricant film thickness in sliding Bearings with overlapped echoes." Tribology International, Volume 88, August 2015, Pages 89-94.

[14] Sen CONG, Tie GANG. "Ultrasonic thickness measurement for aluminum alloy irregular surface parts based on spectral analysis." Transactions of Nonferrous Metals Society of China, Volume 22, Supplement 2, December 2012, Pages s323-s328.

[15] Shao Jiang Wang, Li Hou, Yu Lin Wang, Jian Quan Zhang. "Noise Reduction Using Wavelet Transform in Ultrasonic Flaw Detection of Small-Diameter Steel Pipe with Thick Wall." Advanced Materials Research , 2012 , 383-390 (2) :4755-4761

[16] Brekhovskikh LM. Waves in Layered Media. New York: Academic; 1960

[17] Ali Bulent Koc, Mustafa Vatandas. "Ultrasonic velocity measurements on some liquids under thermal cycle: Ultrasonic velocity hysteresis." Food Research International, Volume 39, Issue 10, December 2006, Pages 1076-1083.

[18] Ling Xie. "The Heat load Prediction Model based on BP Neural Network-markov Model." Procedia Computer Science, Volume 107, 2017, Pages 296-300.

[19] Dongliang Ma, Tao Zhou, Jie Chen, Shi Qi, Zejun Xiao. "Supercritical water heat transfer coefficient prediction analysis based on BP neural network." Nuclear Engineering and Design, Volume 320, 15 August 2017, Pages 400-408.

[20] Bing Wu, Shaojun Han, Jin Xiao, Xiaoguang Hu, Jianxin Fan. "Error compensation based on BP neural network for airborne laser ranging", Optik - International Journal for Light and Electron Optics, Volume 127, Issue 8, April 2016, Pages 4083-4088.

[21] Li-juan HUANG, Xiao-qing GAN. "Customers' Clustering Analysis and Corresponding Marketing Strategies based on Improved SOFM ANN in e-Supply Chain". Systems Engineering - Theory & Practice, Volume 27, Issue 12, December 2007, Pages 49-55.
[22] Yong-zheng JIANG, Hua-ping TANG. "Method for Improving Transverse Wall Thickness Precision of Seamless Steel Tube Based on Tube Rotation". Journal of Iron and Steel Research, International, Volume 22, Issue 10, October 2015, Pages 924-930.
[23] Wei He, Yuncheng Ouyang and Jie Hong, "Vibration Control of a Flexible Robotic Manipulator In the Presence of Input Deadzone", IEEE Transactions on Industrial Informatics, vol. 13, no. 1, pp. 48–59, 2017.
[24] Wei He, Yuhao Chen and Zhao Yin, "Adaptive Neural Network Control of an Uncertain Robot with Full-State Constraints", IEEE Transactions on Cybernetics, vol. 46, no. 3, pp. 620-629, 2016.

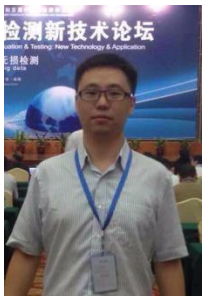

Xiang Xiao received the B.Sc. degree in Automation and the M.Sc. degree in Detection Technology and Automation Device from the Southwest University of Science and Technology and Hunan University, in 2004 and 2007, respectively. He is currently working toward the Ph.D. degree in non-destructive test using infrared thermography, ultrasound and data fusion at UESTC, Chengdu, China.,

Bin Gao (M' 12-SM' 14) received his B.Sc. degree in communications and signal processing from Southwest Jiao Tong University (2001-2005), China, MSc degree in communications and signal processing with Distinction (2006-2007) and PhD degree from Newcastle University, UK (2007-2011). He worked as a Research Associate (2011-2013) with the same university on wearable acoustic sensor technology. Currently, he is a Professor with the School of Automation Engineering, University of Electronic Science and Technology of China (UESTC), China. His research interests include sensor signal processing, machine learning, social signal processing, nondestructive testing and evaluation where he actively publishes in these areas. He has published over 60 papers on these topics on various journals and international conference proceedings. He has coordinated several research projects from National Natural Science Foundation of China.

Gui Yun Tian (M'01-SM'03) received the B.Sc. degree in metrology and instrumentation and M.Sc. degree in precision engineering from the University of Sichuan, Chengdu, China, in 1985 and 1988, respectively, and the Ph.D. degree from the University of Derby, Derby, U.K., in 1998. From 2000 to 2006, he was a Lecturer, Senior Lecturer, Reader, Professor, and Head of the group of Systems Engineering, respectively, with the University of Huddersfield, U.K. Since 2007, he has been based at Newcastle University, Newcastle upon Tyne, U.K., where he has been Chair Professor in Sensor Technologies. Currently, He is also an adjunct professor with School of Automation Engineering, University of Electronic Science and Technology of China. He has coordinated several research projects from the Engineering and Physical Sciences Research Council (EPSRC), Royal Academy of Engineering and FP7, on top of this he also has good collaboration with leading industrial companies such as Airbus, Rolls Royce, BP, nPower, Networkrail and TWI.

Yi Cheng Zhang received a Ph.D. from Wuhan University in 2012. He is engaged in signal processing algorithm research.

Shu Chen received the M.Sc. degree in Control Theory and Engineering from the Huazhong University of Science and Technology in 2007. He is currently working toward the automatic control.